Porosity control in metal-assisted chemical etching of degenerately doped silicon nanowires

2012 Nanotechnology 23 305304

(http://iopscience.iop.org/0957-4484/23/30/305304)

Nanotechnology **23** (2012) 305304 (7pp) doi:10.1088/0957-4484/23/30/305304

Porosity control in metal-assisted chemical etching of degenerately doped silicon nanowires

Karthik Balasundaram[1], Jyothi S Sadhu[2], Jae Cheol Shin[1], Bruno Azeredo[2], Debashis Chanda[3], Mohammad Malik[1], Keng Hsu[2], John A Rogers[3], Placid Ferreira[2], Sanjiv Sinha[3] and Xiuling Li[1]

[1] Department of Electrical and Computer Engineering, University of Illinois, Urbana Champaign, IL 61801, USA
[2] Department of Mechanical Science and Engineering, University of Illinois, Urbana Champaign, IL 61801, USA
[3] Department of Material Science and Engineering, University of Illinois, Urbana Champaign, IL 61801, USA

E-mail: xiuling@illinois.edu and sanjiv@illinois.edu

Received 14 March 2012, in final form 21 May 2012
Published 10 July 2012
Online at stacks.iop.org/Nano/23/305304

Abstract
We report the fabrication of degenerately doped silicon (Si) nanowires of different aspect ratios using a simple, low-cost and effective technique that involves metal-assisted chemical etching (MacEtch) combined with soft lithography or thermal dewetting metal patterning. We demonstrate sub-micron diameter Si nanowire arrays with aspect ratios as high as 180:1, and present the challenges in producing solid nanowires using MacEtch as the doping level increases in both p- and n-type Si. We report a systematic reduction in the porosity of these nanowires by adjusting the etching solution composition and temperature. We found that the porosity decreases from top to bottom along the axial direction and increases with etching time. With a MacEtch solution that has a high [HF]:[H_2O_2] ratio and low temperature, it is possible to form completely solid nanowires with aspect ratios of less than approximately 10:1. However, further etching to produce longer wires renders the top portion of the nanowires porous.

(Some figures may appear in colour only in the online journal)

1. Introduction

Semiconductor nanostructures with high aspect ratios have attracted considerable research interest as promising candidates for improving the cost and performance of several types of devices. In particular, high aspect ratio silicon (Si) nanowires or nanopillars are continuously explored for applications in photovoltaics [1–7], energy storage [8], chemical and bio-sensing [9], thermoelectric modules [10], etc.

Several approaches, both top-down and bottom-up, have been developed for controlled fabrication of silicon nanostructures. Metal-assisted chemical etching (MacEtch) of silicon is a simple and low-cost method offering better controllability of structural parameters such as diameter, length, orientation, morphology, porosity, etc [11–13]. The technique uses a combination of an oxidant (e.g. H_2O_2) and an acid (e.g. HF) with a noble metal (e.g. Au, Ag, or Pt) as the catalyst. Under appropriate etching conditions, the oxidant injects holes through the metal–semiconductor interface to oxidize the semiconductor layer underneath and the acid dissolves the oxidized semiconductor into soluble products. As a result, the metal descends into the semiconductor, producing a three-dimensional semiconductor structure. Silicon nanowires can be formed by using a metal mesh pattern on silicon through MacEtch.

Recent measurements [10] claim that silicon nanowires made using MacEtch possess room temperature thermal

conductivity 5–15 times smaller compared to wires of similar dimensions fabricated using the vapor–liquid–solid growth technique. Experimentally, there appears to be little impact of the roughness on charge transport. The claimed figure of merit is two orders of magnitude larger than bulk silicon and is competitive with telluride compounds. However, silicon must be doped in excess of 10^{19} cm^{-3} to obtain peak power factors in thermoelectrics [14]. This poses a significant challenge in processing nanowires made using MacEtch since higher doping is known to introduce porosity that may effectively reduce the power factor.

Several groups have reported on the effect of Si dopant types and doping levels on the MacEtch rate and the resulting silicon morphology. In general, it has been found that highly doped silicon wafers have the tendency to form porous instead of solid nanowires. Cruz *et al* [15] reported the Au-MacEtch behavior of p-type silicon as a function of dopant concentration and attributed the formation of the porous structure in degenerately doped silicon to the diffusion of excess holes from the Si/Au interface to the off-metal areas. Highly doped n-type nanowires from Ag-MacEtch reported by Schade *et al* [16] were porous, comprising of single crystalline silicon surrounded by amorphous silicon and silicon suboxides. Recently, Hochbaum *et al* [17] also reported single crystalline mesoporous silicon nanowires from MacEtch of degenerately doped wafers using silver nitrate and HF. Their work found that the porosity increases with silicon dopant concentrations under the same etching condition. Although Zhang *et al* [9] achieved non-porous silicon nanowires for highly doped (resistivity = 0.003–0.005 Ω cm) wafers using Ag-MacEtch, the wires had diameters that were smaller when compared to the wires made from lightly doped wafers. It is imperative to further explore the MacEtch parameter space in order to gain insights into controlling the porosity of degenerately doped silicon.

In this paper, we report a systematic study of the Au-MacEtch behavior of degenerately doped p-type and n-type silicon to produce nanowires from sub-micron to sub-100 nm in diameter under various MacEtch conditions, including the effect of etchant concentration, etch temperature, and time evolution. We analyze the possibilities and limitations of MacEtch of silicon wafers that are doped degenerately.

2. Experimental section

In our experiments, we used two different types of metal patterning methods to produce nanowires of different ranges of diameters. Soft lithography [18] was used to form Au mesh patterns in the size range of 200–800 nm, which results in ordered arrays of nanowires of the same diameter as the Au mesh. The lower limit of diameter of the produced nanowires (200 nm in this paper) is limited by the reproducibility of the gold mesh patterns produced by the soft lithography technique. A new patterning method that involves silver metal film dewetting on the silicon surface to form small Ag nanoparticles, followed by Au evaporation on this Ag template and subsequent Ag liftoff was used to produce Au mesh with hole dimensions in the range 60–100 nm and area coverage of 30–40% [19].

Highly doped (100) p-type wafers with a resistivity in the range of 0.0005–0.005 Ω cm, and n-type wafers with a resistivity of 0.001–0.01 Ω cm were used for this study. For soft lithography patterning, a layer of SiN_x was first deposited on top of the silicon wafer, followed by a spin-coated layer of SU-8. Using a PMMA stamp, the pattern was imprinted onto the SU-8. Next the depressed SU-8 was removed using an oxygen plasma etch. The sample was then subject to a CHF_3 etch to remove the exposed SiN_x. The SU-8 patterns made using soft lithography [20] were rinsed with 50:1 buffered oxide etch (BOE) solution for 1 min before evaporating the metal. This step is to ensure a clean metal–semiconductor interface which is critical for MacEtch. Next, a thin layer (20 nm) of Au was deposited which was followed by metal liftoff in Piranha solution (3:1 mixture of 98% sulfuric acid and 30% hydrogen peroxide) for 10–15 min. After the metal liftoff process, the wafers were rinsed with deionized water and blown dry with nitrogen. The wafers were cleaved into samples of dimensions 1 cm × 1 cm for etching.

To produce highly doped p-type nanowires, we varied the volumetric ratio of HF to H_2O_2 as follows: 1:1, 2:1, 3:1, 5:1, 7:1, 10:1, 15:1, 20:1, 25:1 and 30:1. In the first set of experiments, we kept the volume of ethanol the same as that of HF. In the second set of experiments, we kept a constant 10:1 ratio of [HF] to [H_2O_2] and varied the volume of ethanol from 1, 2, 3, 5, 6 and 10 parts per volume of HF. In the case of highly doped n-type nanowires, we tried three different volumetric ratios of HF to H_2O_2, namely 10:1, 15:1 and 20:1, keeping the volume of ethanol as six parts per volume of HF (volumes lower than six parts had issues with metal peeling off).

3. Results and discussions

It has been shown previously that for silicon wafers with a resistivity of 1–10 Ω cm, the etchant concentration used in Ag-MacEtch has a significant impact on the resulting nanowire morphology (solid versus porous) and orientation (vertical or slanted) [21]. It was also reported that for the same MacEtch solution concentration, the porosity of silicon nanowires produced varies depending on the silicon wafer doping level [17]; and porous silicon nanowires with a conical shape were formed for highly doped silicon using Au-MacEtch [22]. Much different MacEtch solution concentrations are thus required to produce vertical and solid nanowires from highly doped wafers. Shown in figure 1 are the tilted top view SEM images of highly doped p-type (resistivity = 0.001–0.01 Ω cm) and n-type (resistivity = 0.001–0.01 Ω cm) silicon nanowire arrays with different diameters produced by Au-MacEtch using the Au mesh pattern produced by soft lithography. The MacEtch concentrations ([HF]/[H_2O_2]/[Ethanol]) used were 5:1:1 and 10:1:1 for p^+ and n^+ silicon wafers, respectively. It should be noted that the 5:1:1 recipe did not lead to significant etching for n^+ silicon. All but 200 and 550 nm diameter n^+ silicon nanowires are vertical with a solid appearance under

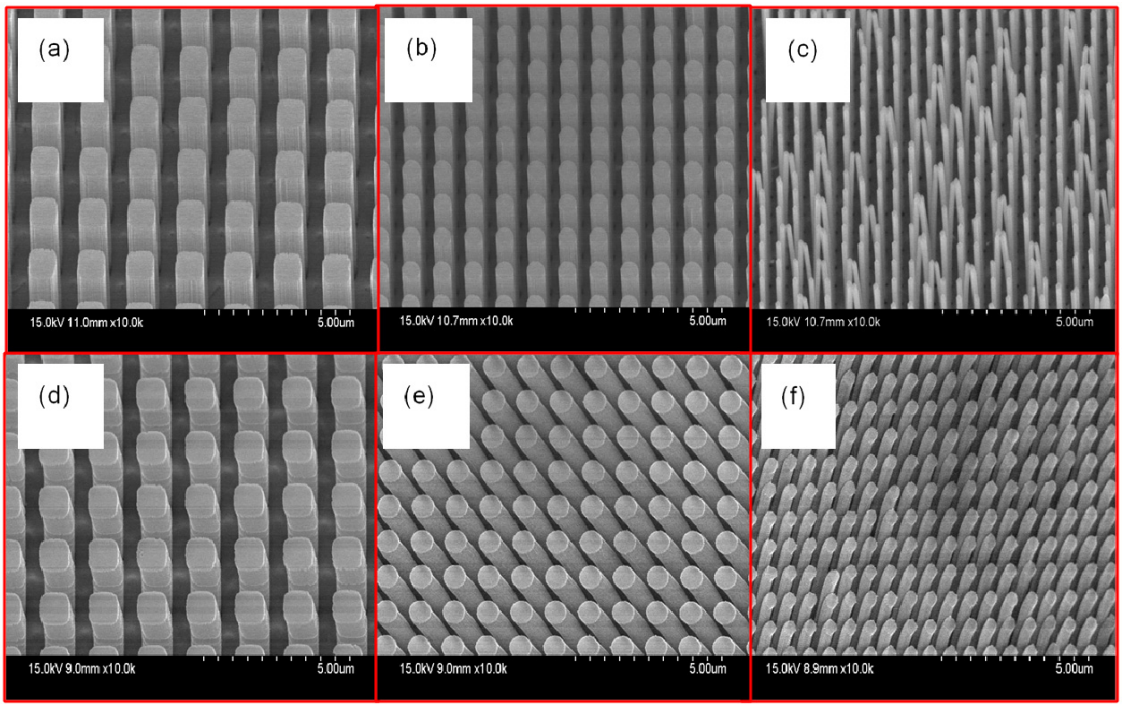

Figure 1. SEM images of p^+ (resistivity = 0.001–0.01 Ω cm) and n^+ (resistivity = 0.001–0.01 Ω cm) nanowire arrays produced by Au-MacEtch with Au mesh patterned by soft lithography. (a)–(c) 45° tilted view of p^+ nanowires of 800, 550, and 200 nm in width/diameter, respectively, produced by the 5:1:1 ([HF]/[H_2O_2]/[ethanol]) recipe; (d)–(f) 45° tilted view of n^+ nanowires of 800, 550, and 200 nm in width/diameter, respectively, produced by the 10:1:1 recipe.

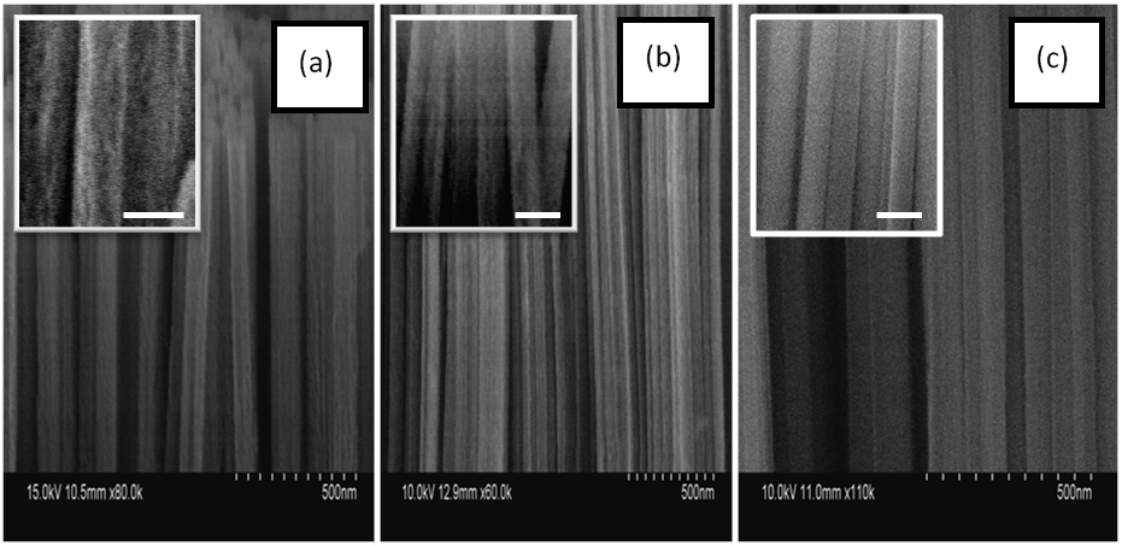

Figure 2. SEM images of sidewalls of p^+ nanowires (resistivity = 0.001–0.005 Ω cm and diameter ∼60–80 nm) formed with dewetting Au patterns using [HF]/[H_2O_2]/[ethanol] recipes of (a) 3:1:3 (b) 7:1:7 and (c) 10:1:10 respectively. The inset shows high magnification SEM images of sidewalls of nanowires indicating a reduction in porosity from (a) to (c). The scale bar is 200 nm.

the specified magnification with these etching conditions. In contrast to MacEtch of lightly doped silicon wafers, the HF concentration needed is much higher, in other words, a lower concentration of H_2O_2 (oxidant) is required. It should also be noted that the same concentration range would lead to no pattern formation but electropolishing for lightly doped silicon wafers [21].

To examine if the produced silicon nanowires are truly solid, we have systematically characterized the nanowires produced from p^+ silicon using MacEtch solutions with [HF]:[H_2O_2] volume ratios from 3:1 to 30:1 by SEM and TEM. Figures 2(a)–(c) show the SEM images of highly doped (resistivity = 0.001–0.005 Ω cm) p-type nanowires fabricated using 3:1, 7:1 and 10:1 [HF]:[H_2O_2], respectively (the volume

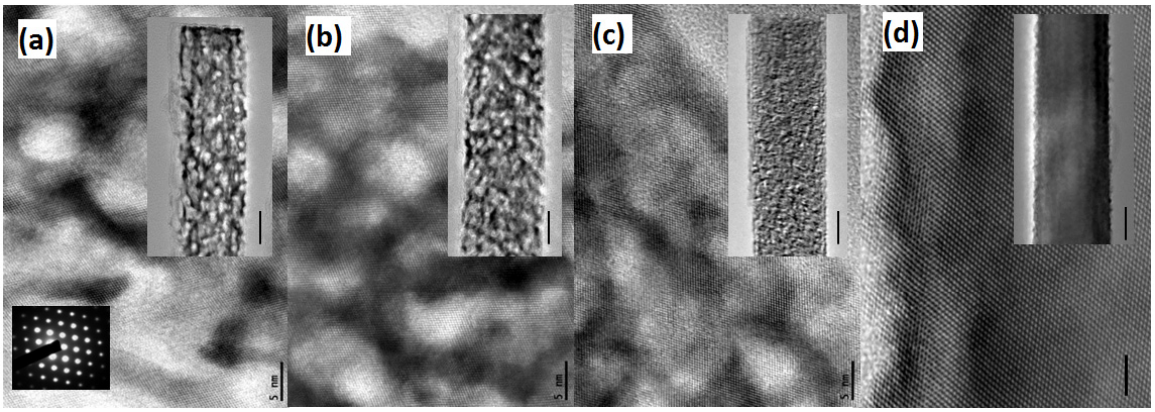

Figure 3. Degree of porosity of degenerately doped p-type nanowires under different etch concentrations. p^+ nanowires (resistivity = 0.001–0.005 Ω cm and diameter ∼60–80 nm) from the dewetting pattern made using the [HF]:[H_2O_2] volumetric ratio of (a) 10:1 at room temperature, (b) 20:1 at room temperature, and (c) 30:1 at room temperature, and (d) shows the TEM images of solid wires made from lightly doped silicon (resistivity = 10 Ω cm and diameter ∼100 nm) for comparison. The inset shows the SAED pattern (a) from p^+ nanowires and HRTEM images (scale bar = 50 nm) of the nanowire.

of ethanol was kept the same as the volume of HF in all cases). The high magnification SEM images of the nanowire arrays etched using 3:1 [HF]: [H_2O_2] MacEtch solutions (figure 2(a)) clearly show the presence of pores. The porosity decreases with increasing [HF]:[H_2O_2] ratio. For concentration ratios greater than 7:1 (figure 2(c)), the porosity shows a significant reduction and appears to approach a nearly solid morphology within the resolution of the SEM.

However, under TEM (figure 3(a)), it is apparent that pores, which appear as phase contrast in the TEM image, are still present when the 10:1 MacEtch solution is used. In order to systematically study the porosity control, we record high resolution transmission electron micrographs (HRTEM) of the nanowires by tilting to the [110] zone axis. We observe several regions in the interior of the nanowires where the lattice fringes are absent, indicating the presence of the pores. The selected area electron diffraction (SAED) pattern confirms the single crystalline nature of the etched wires. A further reduction of the porosity has been found with continuously increasing [HF] as shown in figures 3(b) and (c). The analysis of images also reveals that the maximum diameter of pores reduces with [HF]:[H_2O_2] ratio from 11 nm (10:1), to 8 nm (20:1) to 5 nm (30:1). It is clear that the nanowires are single crystalline and the porosity at the 30:1 ratio of [HF]:[H_2O_2] (figure 3(c)) is dramatically reduced, even though some porosity still remains in contrast to the fully solid nanowires fabricated using MacEtch from lightly doped p-type (resistivity = 10 Ω cm) silicon wafers (figure 3(d)). It should be noted that since HRTEM images are a two-dimensional projection of several atomic planes of the nanowire, it is not straightforward to calculate the average level of porosity from these images.

The formation of high aspect ratio nanostructures with a porous morphology using MacEtch has been attributed to the diffusion of holes outside of the metal–semiconductor interface and causing an additional but reduced extent of etching in the areas outside the metal mesh pattern [14]. Hochbaum *et al* [17] reported an increase in the porosity of p-type silicon nanowires with increasing dopant concentration when etched under the same MacEtch concentration. Their work stated that hole transport (thus, pore formation) is more favorable due to less band bending at the metal–semiconductor interface for highly doped wafers. Our experiments here provide an understanding of the role of relative concentrations of the acids and oxidants in the MacEtch solution for silicon wafers at a specific high doping level. We hypothesize that at a very high [HF]:[H_2O_2] ratio (e.g. 30:1), the hole generation process dominates the etch rate and thus there is little time for the injected holes to diffuse before HF removal of Si^{4+}. In other words, increasing the rate of Si^{4+} removal with a higher [HF]:[H_2O_2] ratio can help to reduce hole transport and thus the formation of pores. The complete model for porous silicon formation from degenerately doped wafers should include both the energy barrier model [17] and the exact [HF]:[H_2O_2] ratio [21] for a given crystal orientation. In our studies, we have shown the etching mechanism only for (100) silicon wafers which are degenerately doped to both p-type and n-type.

In addition to [HF], we have found that the etch time changes the porosity too. Previously, Qu *et al* [23] reported an increase in porosity of n^+ nanowires made using silver-assisted chemical etching when they increased the etch time from 30 to 60 min. Under our Au-MacEtch condition, the same trend in porosity has been found in a matter of 30 versus 60 s etching time using the 15:1 ([HF]:[H_2O_2]) recipe for n^+ silicon nanowires. We have also observed a gradual change in porosity along the axis of the nanowire produced by MacEtch from these highly doped silicon wafers. In figure 4, we have shown the TEM images of three segments of a nanowire produced from an n^+ silicon wafer using the [HF]:[H_2O_2] ratio of 10:1 after etching for 3 min. A gradual increase in porosity along the axial length (∼3 μm) of the nanowire can be clearly seen. Note that this is different from the change in porosity along the axial direction by intentionally changing the [H_2O_2] during etching as reported by Chiappini *et al* [24]. In our etching process, we have kept the same concentration of

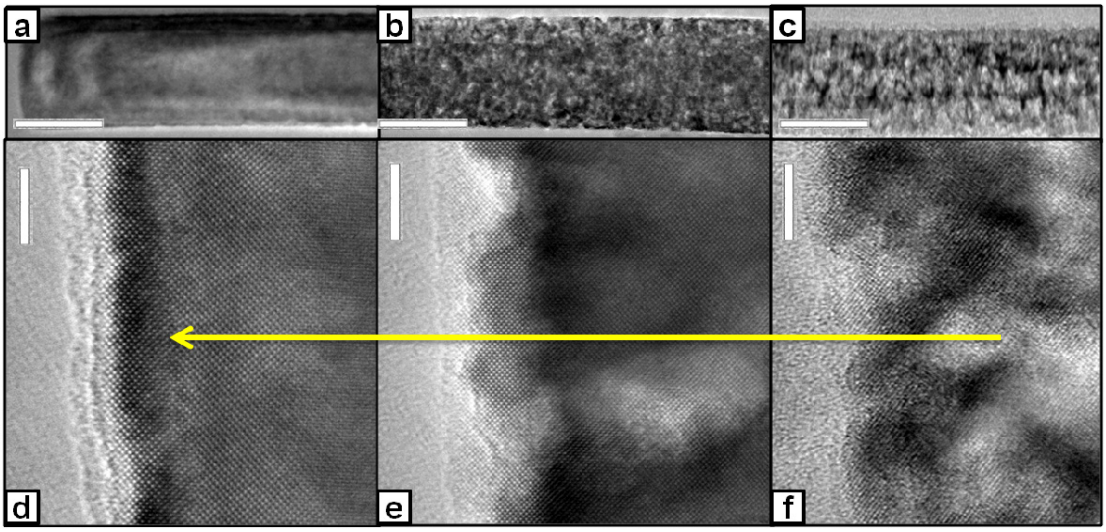

Figure 4. Axial variation of porosity of n-type degenerately doped wires. Low resolution TEM images of an n^+ wire (resistivity = 0.001–0.01 Ω cm) etched using the [HF]/[H_2O_2]/[ethanol] ratio of 10:1:6 for 3 min showing the (a) bottom, (b) middle and (c) tip regions of the nanowire. (d)–(f) shows the corresponding HRTEM images and the arrow indicates the etch direction. Scale bars for (a)–(c) and (d)–(f) are 50 nm and 5 nm, respectively.

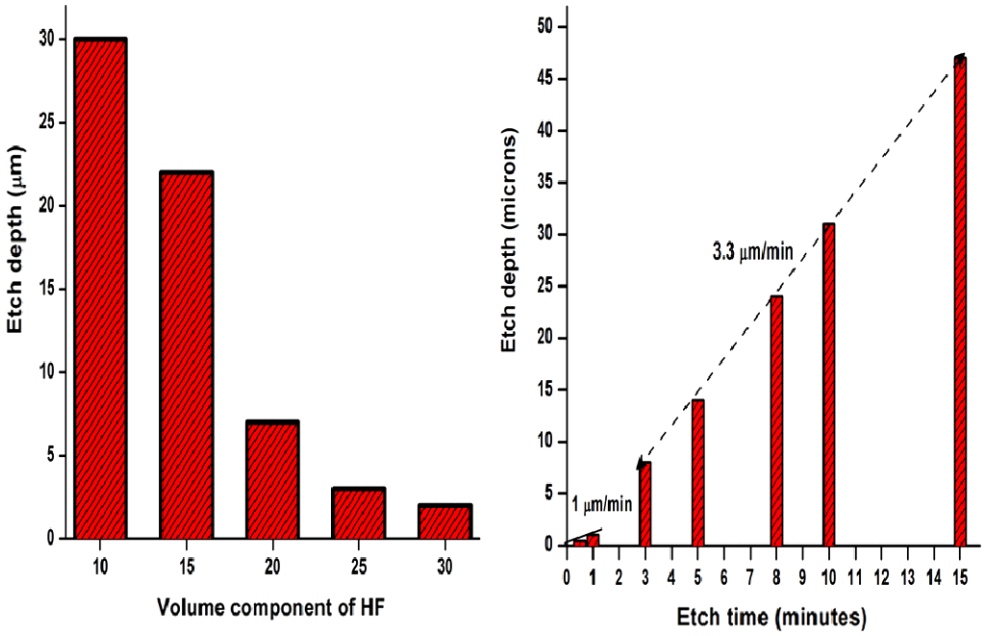

Figure 5. Variation of etch rate with chemical composition and etch time. (Left) Etch depth as a function of volume component (x) of HF for p^+ (resistivity = 0.001–0.005 Ω cm and diameter ∼60–80 nm) nanowires etched for 10 min in x:1:3 ([HF]/[H_2O_2]/[ethanol]) recipes. The etch depth decreases with higher volume components of HF. (Right) Etch depth as a function of etch time for 60–80 nm p^+ nanowires produced using the 10:1:3 ([HF]/[H_2O_2]/[ethanol]) recipe. The variation of etch depth follows a linear trend (as shown by the dashed line with arrows) after the first few minutes.

etchants during the entire duration. The decrease in porosity along the axis from the top to bottom of the wires may be due to the prolonged exposure of the tip and the middle parts of the wires in the etching solution. As the etching proceeds downwards, the dopant atoms inside the top and middle portions of the wires which are thermodynamically favorable sites for the formation of pores [17] are subjected to longer exposure to etchants and hence we observe a gradual change in the porosity as shown in the low and high resolution TEM images in figure 4.

Not surprisingly, increasing the [HF] in the solution decreases the etch rate. As shown in figure 5, there is a quadratic trend in the etch depth of p^+ silicon nanowires with increasing [HF] from 10, 15, 20, 25 to 30 volume by parts. All the samples were etched for a period of 10 min at room temperature. All SEM and TEM images from figures 2

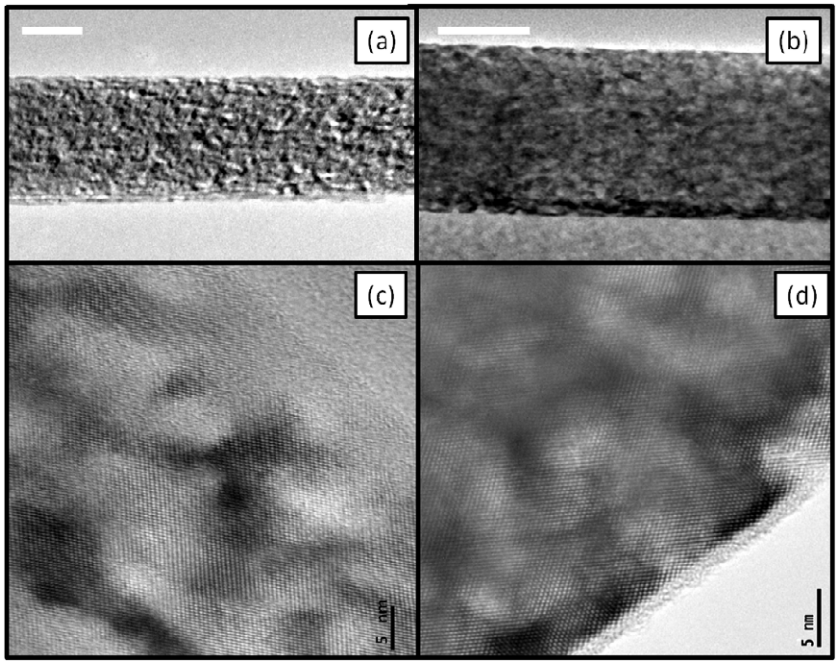

Figure 6. Effect of etch temperature on porosity. Comparison of TEM images of p^+ (resistivity = 0.001–0.005 Ω cm and diameter ∼60–80 nm) nanowires etched using the [HF]/[H_2O_2]/[ethanol] ratio of 30:1:1 at different conditions—((a) and (c)) room temperature and ((b) and (d)) low temperature using an ice bath (0 °C) with a nanowire length ∼3 μm. The wire boundary is also shown. The scale bars for (a)–(b) and (c)–(d) are 50 nm and 5 nm, respectively.

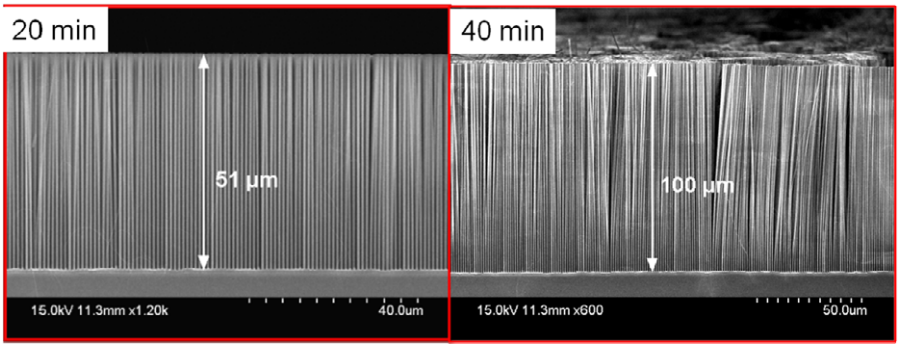

Figure 7. Demonstration of vertical high aspect ratio nanopillars without supercritical drying. Cross-sectional SEM image of p^+ nanopillars (resistivity = 0.0005–0.001 Ω cm and diameter = 550 nm) etched for (left) 20 min and (right) 40 min using soft lithography and the [HF]/[H_2O_2]/[ethanol] ratio of 5:1:1.

and 3 were obtained from nanowires of the same length at approximately the same location near the top.

To study the etch rate dependence over time, we varied the duration of etching from 30 s to 15 min using the 10:1:3 recipe for the p^+ nanowires made using the dewetting technique with diameters ∼60–80 nm. As shown in figure 5(b), the initial etch rate is ∼1 μm min^{-1}, and then it increases to ∼3 μm min^{-1}, as reflected by the slope of the fitted line, after approximately a minute and remains the same thereafter. We believe this change in etch rate after the first few seconds may be due to the presence of a thin layer of non-silicon material such as silicon suboxides (SiO_x) formed during the metal patterning step which retards the injection of holes from the metal during the initial stage of the reaction and gradually gets dissolved by HF during the course of the reaction. We also observed an absence of any change in color of the metal layer during the initial few seconds after dipping the sample into solution. This absence of any visible color change (an indicator of MacEtch reaction due to diffraction from produced 3D structures) which implies a very sluggish etching process further supports the measured etch rate.

All MacEtch results above were carried out at room temperature. We have found that when the etching temperature decreases, the porosity is reduced. Shown in figures 6(a) and (b) are TEM images taken from wires fabricated using the 30:1 volumetric ratio of HF and H_2O_2 at room temperature and 0 °C (ice bath), respectively. From the low resolution TEM images of the wires shown in figures 6(a) and (b), we found that the nanowires made using the ice bath (0 °C) had a pronounced decrease of phase contrast when

compared to those made at room temperature and also had a relatively smooth sidewall morphology. We attribute this trend to the reduced rate of diffusion of injected holes into off-metal areas. The etch rate for these wires was found to be around 125–150 nm min^{-1} at 0 °C which is six or seven times lower than the etch rate (800–1000 nm min^{-1}) at room temperature using the same 30:1 ratio of HF and H_2O_2. Our method on low temperature metal-assisted chemical etching of degenerately doped silicon nanowires shows a new dimension in the parameter space of controlling the porosity of nanowires. This reduction in porosity also implies that further lowering the temperature may readily lead to completely solid nanowires.

Shown in figure 7 are p^+ silicon nanopillars (resistivity = 0.0005–0.001 Ω cm) of diameter 550 nm formed using the 5:1:1 recipe for 20 and 40 min. The height ranges from 51 to 100 μm, which corresponds to a change in aspect ratio of 92–182, respectively. All these nanopillars are vertical and highly uniform throughout the array. Chang *et al* [25] reported an aspect ratio of 220 of silicon nanowires (∼20 nm diameter) subjected to critical point drying (CPD) to minimize the cluttering at the tips of nanowires due to surface tension. Remarkably, the high aspect ratio nanowire arrays in figure 7 were fabricated without CPD. Instead, we rinsed the nanopillars in the following sequence: deionized water, methanol and deionized water for 1 min each and baked the samples on a hot plate at 60–80 °C after the MacEtch process. These steps help to ensure that the nanopillars do not get cleaved or cluttered, which occurs commonly for drying processes using an inert gas.

4. Conclusions

In summary, we have fabricated degenerately doped p-type and n-type nanowires of dimensions ranging from sub-micron to sub-100 nm using MacEtch. We have reported the effect of the [HF] to [H_2O_2] ratio, etch time and temperature on the etch rate and porosity of the fabricated nanowires. High [HF]:[H_2O_2], low temperature, and shorter etching time are some factors that help to reduce the porosity. It is possible to achieve solid and vertical degenerately doped nanowires with ∼1 μm in height and diameter ∼60–80 nm (aspect ratio ∼10:1). The etching direction, reduction of porosity and etch rate have been explained based on the hole transport into off-metal areas during etching. In addition, we have shown a simple method to fabricate high aspect ratio nanopillars (∼180:1) without any complicated post-processing steps such as supercritical drying. The demonstrated control over porosity is especially important for thermoelectric applications. Measurements of transport properties in these wires can further elucidate if the range of control is sufficient to obtain peak power factors similar to bulk silicon and perhaps even improve the figure of merit through additional phonon scattering. Our results on the fabrication of high aspect ratio degenerately doped silicon nanostructures with tunable porosity using the simple, low-cost MacEtch technique advance the potential use of such nanowires in energy harvesting, storage and sensing applications.

Acknowledgments

This work was supported in part by DOE DE-AR0000041 ARRA, DOE DEFG02-07ER46471 through the Frederick Seitz Materials Research Laboratory at the University of Illinois at Urbana-Champaign and the NSF under award no. 0749028 (CMMI).

References

[1] Fang H, Li X, Song S, Xu Y and Zhu J 2008 *Nanotechnology* **19** 255703
[2] Shu Q *et al* 2009 *Nano Lett.* **9** 4338–42
[3] Peng K, Wang X and Lee S-T 2008 *Appl. Phys. Lett.* **92** 163103
[4] Peng K-Q and Lee S-T 2011 *Adv. Mater.* **23** 198–215
[5] Shu Q *et al* 2010 *Chem. Commun.* **46** 5533–5
[6] Peng K, Xu Y, Wu Y, Yan Y, Lee S-T and Zhu J 2005 *Small* **1** 1062–7
[7] Garnett E C and Yang P 2008 *J. Am. Chem. Soc.* **130** 9224–5
[8] Peng K, Jie J, Zhang W and Lee S-T 2008 *Appl. Phys. Lett.* **93** 033105
[9] Zhang B, Wang H, Lu L, Ai K, Zhang G and Cheng X 2008 *Adv. Funct. Mater.* **18** 2348–55
[10] Hochbaum A I, Chen R, Delgado R D, Liang W, Garnett E C, Najarian M, Majumdar A and Yang P 2008 *Nature* **451** 163–7
[11] Li X and Bohn P W 2000 *Appl. Phys. Lett.* **77** 2572–4
[12] Huang Z, Geyer N, Werner P, de Boor J and Gösele U 2011 *Adv. Mater.* **23** 285–308
[13] Li X 2011 *Curr. Opin. Solid State Mater. Sci.* **16** 71–81
[14] Geballe T and Hull G W 1955 *Phys. Rev.* **98** 940–7
[15] Cruz S, Hönig-d'Orville A and Müller J 2005 *J. Electrochem. Soc.* **152** C418
[16] Schade M, Geyer N, Fuhrmann B, Heyroth F and Leipner H S 2009 *Appl. Phys.* A **95** 325–7
[17] Hochbaum A I, Gargas D, Hwang Y J and Yang P 2009 *Nano Lett.* **9** 3550–4
[18] Shir D, Yoon J, Chanda D, Ryu J-H and Rogers J a 2010 *Nano Lett.* **10** 3041–6
[19] Azeredo B P D *et al* 2012 private communication
[20] Zaumseil J, Meitl M A, Hsu J W P, Acharya B R, Baldwin K W, Loo Y-L and Rogers J A 2003 *Nano Lett.* **3** 1223–7
[21] Chern W, Hsu K, Chun I S, Azeredo B P D, Ahmed N, Kim K H, Zuo J, Fang N, Ferreira P and Li X 2010 *Nano Lett.* **10** 1582–8
[22] Mikhael B, Elise B, Xavier M, Sebastian S, Johann M and Laetitia P 2011 *ACS Appl. Mater. Interfaces* **3** 3866–73
[23] Qu Y, Liao L, Li Y, Zhang H, Huang Y and Duan X 2009 *Nano Lett.* **9** 4539–43
[24] Chiappini C, Liu X, Fakhoury J R and Ferrari M 2010 *Adv. Funct. Mater.* **20** 2231–9
[25] Chang S-W, Chuang V P, Boles S T, Ross C A and Thompson C V 2009 *Adv. Funct. Mater.* **19** 2495–500